

Numerical Study Of Natural Convective Heat Transfer In An Inclined Square Porous Layer

Amir S. Dawood

Muyassar E. Ismaeel

Department of Mechanical Engineering, Mosul University

Abstract

In this paper, steady two-dimensional natural convective heat transfer in an inclined square porous cavity with two parallel walls kept at constant different temperatures, while the other two parallel walls were well insulated, has been studied numerically. The governing equations have been solved using finite difference method. Results have been obtained for modified Rayleigh numbers between 0 and 300 and inclination angle between 0° (heated from below) and 90° (heated from side). The rate of heat transfer was found a strong function of modified Rayleigh number and inclination angle. The maximum heat transfer was occurred at about ($50^\circ \leq \phi \leq 57^\circ$) degrees of inclination.

Keywords: Natural Convective Heat Transfer, Porous Medium, Inclined Enclosure.

دراسة عددية لانتقال الحرارة بالحمل الطبيعي
في طبقة مسامية مربعة مائلة

ميسر ادريس اسماعيل

أمير سلطان داؤد

قسم الهندسة الميكانيكية/جامعة الموصل

الخلاصة

في هذا البحث ، تم إجراء دراسة عددية لانتقال الحرارة بالحمل الطبيعي المستقر ثنائي البعد في تجويف مسامي مربع الشكل له جداران متوازيان ذو درجات حرارة ثابتة ولكن مختلفة والجداران المتوازيان الآخران معزولان.

حصلت الحلول للمعادلات الحاكمة بطريقة الفروق المحددة. ان معدلات انتقال الحرارة المحسوبة قدمت لعدد رالي المطور Ra^* في المدى (0) الى (300) ولزاوية ميلان ϕ تتغير من (0°) (مسخن من الاسفل) الى (90°) (مسخن من الاعلى). ان الدراسة الحالية بينت ان معدل انتقال الحرارة هو دالة قوية من عدد رالي المطور و زاوية الميلان. كذلك بينت ان اقصى انتقال للحرارة يحدث عند زوايا ميلان حوالي ($50^\circ \leq \phi \leq 57^\circ$).

Received 5 March 2006

Accepted 3 Sep. 2007

Nomenclature

Da	=	Darcy number $= (K/H^2)$
g	=	Acceleration due to gravity, (m/s^2)
H	=	Height of cavity, m
K	=	Permeability of porous medium, (m^2)
k_e	=	Effective thermal conductivity of the porous medium, $(W/m.K)$
L	=	Width of porous cavity, (m)
Nu	=	Nusselt number $= Q / Q_{cond,0}$

P	=	Pressure, (Pa)
Q	=	Heat flow rate, (W)
Q_{con}	=	Conduction heat flow rate, (W)
d		
Ra_H	=	Rayleigh number $=(\rho_o g \beta H^3 \Delta T / \mu \alpha)$
Ra^*	=	Modified Rayleigh number $= Ra_H \cdot Da$
Ra_c	=	Critical Rayleigh number for onset of convection
*		
T	=	Temperature, (K)
ΔT	=	Temperature difference $= T_{ho} - T_{co}$, (K)
u	=	Fluid velocity in x-direction, (m/s)
v	=	Fluid velocity in y-direction, (m/s)
x, y	=	Cartesian coordinates

Greek Symbols

α	=	Thermal diffusivity of porous medium, (m ² /s)
β	=	Thermal coefficient of volumetric expansion, (K ⁻¹)
θ	=	Dimensionless temperature $=(T-T_{co})/(T_{ho}-T_{co})$
μ	=	Dynamic viscosity, (kg/m.s)
ν	=	Kinematic viscosity of fluid, (m ² /s)
ρ	=	Density, (kg/m ³)
ϕ	=	Inclination angle, (deg.)
Ψ	=	Stream function, (m ² /s)

Subscript

c	=	Critical
co	=	Cold wall
e	=	Effective
ho	=	Hot wall
o	=	Reference condition

Superscript

\wedge	=	Dimensionless parameter
----------	---	-------------------------

Introduction

Natural convection is one of the important modes of heat transfer. This phenomenon has been observed in numerous environmental circumstances. It occurs frequently as a result of density inversion caused by either the thermal expansion of a fluid, or the concentration gradients within a fluid system. As in fluid, Natural convection can also happen in a porous medium saturated with a fluid [1]. Natural convection heat transfer in porous enclosures commonly takes place in nature, and engineering and technological applications.

Over the past years, more emphasis is put on natural convection in porous media due to its growing importance in engineering and geophysical areas. A wide variety of two-dimensional situations has been studied. The convective flow of fluid through porous media heated from below is of considerable interest in the study of the behavior of geothermal systems and has been investigated extensively in the past.

Horizontal Cavity

Horton and Rogers in 1945 [2] made early theoretical study of natural convection in a horizontal porous media. In 1948, Lapwood (as published in [3]) determined the criterion for stability of the conduction state of such a layer and suggested in his linear analysis that convection occurs at Rayleigh number above $4\pi^2$. Later on, Katto and Mosuoka in 1967 [3] gave experimental confirmation of the onset of free convection satisfying agreement of the experimental results with the theory was obtained previously.

Inclined Cavity

For situations involving inclined layers, available studies are relatively limited. Bories and Combarous [4] in 1973 carried out an experimental and theoretical study of thermal convection in a sloping porous layer. Similar experiments were conducted by Kaneko et al. in 1974 [1]. They found that inclination of the medium and certain properties of the saturating fluid affect the mode and intensity of convective motions. Also, their experiments show that the critical Rayleigh number for the onset of free convection is less than that predicted by the linear theory (i.e. $Ra \cdot \cos \phi = 4\pi^2$). Oosthuizen and Paul in 1984 [5] performed a numerical study to analyze two-dimensional natural convective flow in a square cavity. The cavity was half-filled with a fluid and half-filled with a porous medium which saturated with the same fluid, the fluid and porous medium layer being separated from each other by an impermeable partition that was parallel to the two heated walls and which offered no resistance to the heat transfer. Their results indicated that at all angles of inclination, the mean heat transfer rate across the divided cavity with the porous medium was very much less than that across an undivided fluid filled cavity, the relative decrease being greatest at angles near that at which the maximum heat transfer rate occurs and at the higher Rayleigh number considered. Inaba et al. in 1988 [6] reported an experimental study of natural convection heat transfer in an inclined rectangular cavity filled with liquid and spherical particles, in which two opposing isothermal walls were kept at different temperatures and other walls were thermally insulated. They conclude

that the contribution of (d/H , ratio of spherical particle diameter to height of the cavity) on Nu was remarked in a small inclination angle (ϕ) and the contribution of (L/H , ratio of width to height of the cavity) was significant near $\phi = 90^\circ$. Mbaye et al. in 1993 [7] performed both analytical and numerical study for natural convection heat transfer in an inclined porous layer bordered by wall with finite thickness and conductivity. Their results obtained in terms of an overall Nusselt number as a function of Rayleigh and Darcy number, angle of inclination of the system, and thickness and conductivity of the bordering wall.

Vertical Cavity

Natural convection in a rectangular porous cavity heated from the side is one of the classical problems of free convection in porous media that have been extensively studied. Chan et al. in 1970 [8] used the Brinkman model to study natural convection in a rectangular cavity of porous media filled with gas that was differentially heated in the horizontal direction. Their numerical computations indicate that the Darcy number dependence was unimportant for most situations. Burns et al. in 1977 [9] examined analytically and numerically convection in a vertical slot filled with porous insulation. The work includes wall injection for both free and forced convection. Their results for no wall injection were in good agreement with previous works. Bejan and Tien in 1978 [10] developed an approximate analytical method for the study of natural convection in a porous layer. Their results show good agreement with those of Burns et al. [9] and others. Bejan in 1983 [11] carried out a numerical study of the effect of internal flow obstructions on heat transfer through a two-dimensional porous layer heated from the side. He found that the flow obstructions have a dominated effect on the heat transfer rate.

In addition to the above review of investigation on a rectangular cavity, there are many studies that deal with other shape problems. There exist a good review of studies under this subject presented by Cheng [12].

In this work, the heat transfer rate and mode of natural convection were determined numerically for the system shown in Figure (1). The hot and cold walls, at temperatures T_{ho} and T_{co} , respectively, make an angle ϕ with the horizontal. The other two walls are insulated. The square cavity is fully filled with a porous material saturated with liquid.

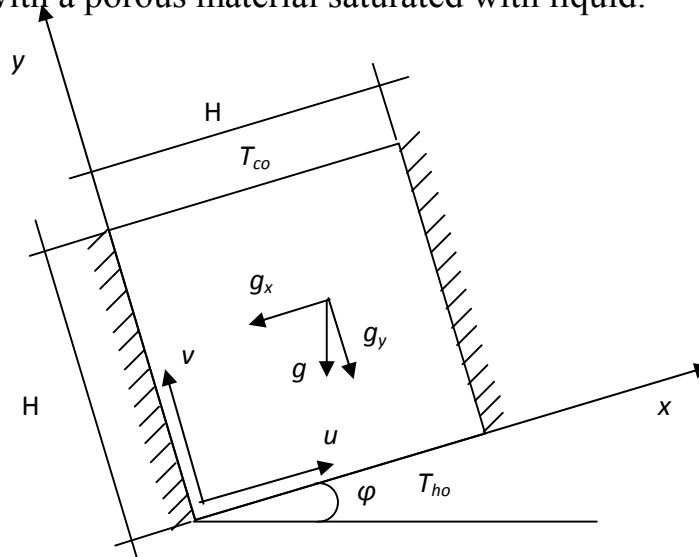


Figure (1) Physical situation and coordinate.

Mathematical Model And Numerical Solution

It has been assumed that the porous matrix is rigid and that the fluid and solid properties are constant except for the density of fluid change with temperature which gives rise to the buoyancy forces, this being treated using Boussinesq approach. It has also been assumed that the fluid and matrix are in thermal equilibrium and that Darcy's law can adequately describe the fluid motion.

The equation of continuity, momentum, and energy transport for two-dimensional and steady state conditions can be expressed, respectively, as:

$$\frac{\partial u}{\partial x} + \frac{\partial v}{\partial y} = 0 \dots\dots\dots(1)$$

$$u = \frac{-K}{\mu} \left(\frac{\partial P}{\partial x} + \rho g \sin \phi \right) \dots\dots\dots(2)$$

$$v = \frac{-K}{\mu} \left(\frac{\partial P}{\partial y} + \rho g \cos \phi \right)$$

.....(3)

$$u \frac{\partial T}{\partial x} + v \frac{\partial T}{\partial y} = \alpha_e \left[\frac{\partial^2 T}{\partial x^2} + \frac{\partial^2 T}{\partial y^2} \right]$$

.....(4)

Further, the pressure terms appearing in equation (2) and (3) can be eliminated through cross-differentiation. By introducing the stream function ψ automatically satisfies equation (1), the governing equations become:

$$\frac{\partial^2 \psi}{\partial x^2} + \frac{\partial^2 \psi}{\partial y^2} = -\frac{\rho_o \beta g K}{\mu} \left[\frac{\partial T}{\partial x} \cos \phi - \frac{\partial T}{\partial y} \sin \phi \right]$$

.....(5)

$$\frac{\partial \psi}{\partial y} \frac{\partial T}{\partial x} - \frac{\partial \psi}{\partial x} \frac{\partial T}{\partial y} = \alpha_e \left[\frac{\partial^2 T}{\partial x^2} + \frac{\partial^2 T}{\partial y^2} \right]$$

.....(6)

Finally, equation (5) and (6) are put in a non-dimensional form by defining a new set of variables.

$$\theta = \frac{T - T_{co}}{T_{ho} - T_{co}} = \frac{T - T_{co}}{\Delta T}, \text{ and } \alpha_e/H$$

All spatial dimensions are non-dimensionalized with respect to H . The resulting equations for the stream function and temperature are:

$$\frac{\partial^2 \hat{\psi}}{\partial \hat{x}^2} + \frac{\partial^2 \hat{\psi}}{\partial \hat{y}^2} = -Ra * \left[\frac{\partial \theta}{\partial \hat{x}} \cos \phi - \frac{\partial \theta}{\partial \hat{y}} \sin \phi \right]$$

.....(7)

$$\frac{\partial \hat{\psi}}{\partial \hat{y}} \frac{\partial \theta}{\partial \hat{x}} - \frac{\partial \hat{\psi}}{\partial \hat{x}} \frac{\partial \theta}{\partial \hat{y}} = \frac{\partial^2 \theta}{\partial \hat{x}^2} + \frac{\partial^2 \theta}{\partial \hat{y}^2}$$

.....(8)

Where, $Ra^* = DaRa = \frac{HKg\beta\Delta T}{v\alpha_e}$ is the modified Rayleigh number, and

$Da = \frac{K}{H^2}$ is the Darcy number.

The boundary conditions on temperature are of Dirichelt and Neumann types and on velocity are of closed type, i.e.:

$$\theta = 1 \quad \text{at} \quad \hat{y} = 0 \quad , \text{ for} \quad 0 \leq \hat{x} \leq \frac{1}{A}$$

.....(9)

$$\theta = 0 \quad \text{at} \quad \hat{y} = 1 \quad , \text{ for} \quad 0 \leq \hat{x} \leq \frac{1}{A}$$

.....(10)

$$\frac{\partial \theta}{\partial \hat{x}} = 0 \quad \text{at} \quad \hat{x} = 0 \quad \text{and} \quad \frac{1}{A} \quad , \text{ for} \quad 0 \leq \hat{y} \leq 1$$

.....(11)

$$\hat{\psi} = 0 \quad \text{on all solid boundaries}$$

.....(12)

To obtain numerical solutions of the complete governing equations (7)

and (8), finite-differences were used. The base of this technique is to approximate all the derivatives in the equation by means of their Taylor series expansions.

The finite-difference approximation scheme used is every where second-order. A central-difference approximation is used for the interior nodes while a one side-difference approximation is used for the boundary nodes. After substituting the above formulas of the finite-difference in the non-dimensional governing equations and re-arranging them in a manner that enable them to be handled by computer, a computer program is written in the FORTRAN language. The iterative procedure for temperature was repeated until the following condition was satisfied:

$$\sum |T_{N_{i,j}} - T_{i,j}| \leq 10^{-4}$$

Before starting the computational solution, the grid independence of the results must be tested. Thus, numerical experiments have been carried out to solve a two-dimensional convection problem in which the angle of inclination $\phi = 0^\circ$. The Rayleigh number in this test is set to be 150, while the grid size varies from 10x10 to 70 x 70. It is found that the change in the heat flow rate for grid size of 60 x 60 and 70 x 70 is less than 0.5 percent. Therefore, the number of grid that is adopted in the present study is 60 x

60. The number of grid was selected as a compromise between accuracy and speed of computation.

The values of average Nusselt number have been compared with those of other investigators using the same boundary conditions to show the validation of the present numerical results. Figure (2) illustrate a comparison between the present results and those of other authors for the case of cavity heated from below, they show a good agreement. On the other hand, Table (1) shows the comparison of Nusselt number for a cavity heated from the side. As a further check on the numerical results, average Nusselt numbers at the hot and cold walls were compared, and they differed by less than 0.6 % in all computer runs. The Nusselt numbers to be presented are those for the hot wall.

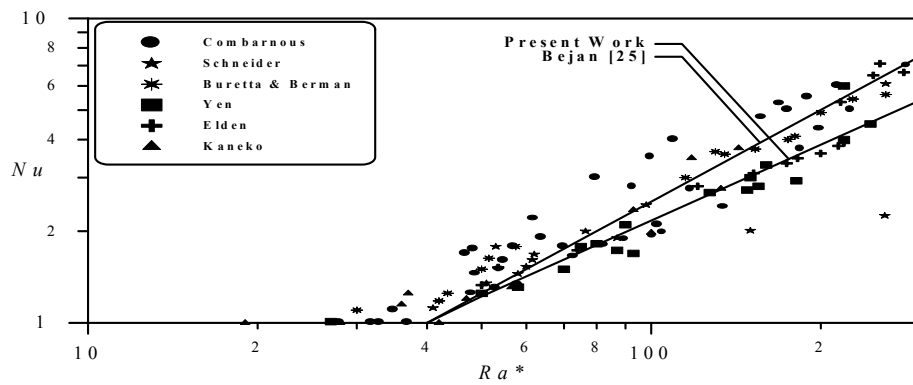


Figure (2) Nusselt number vs. Rayleigh number for a horizontal porous layer heated from below [12].

$$Nu$$

Ra Chan Burns Bejan & Bejan Dawood Present

*	[8]	[9]	Tien [10]	[11]	[13]	Work
50	2.1	2.2	2.12	1.897	2.22	2.034
10	3.54	3.6	3.25	3.433	3.472	3.472
0						

Table (1) Nusselt number comparison for the case of the cavity heated from the side.

Results And Discussion

This article presents the results of the numerical solution of the convective heat transfer in an inclined porous layer. The field and the average Nusselt numbers are presented and discussed as they vary with the investigation parameter (i.e. Rayleigh number $0 \leq Ra \leq 300$ and inclination angle $0^\circ \leq \phi \leq 90^\circ$). Most of the results are presented graphically. Finally, curve fits of the results are presented.

Flow Results

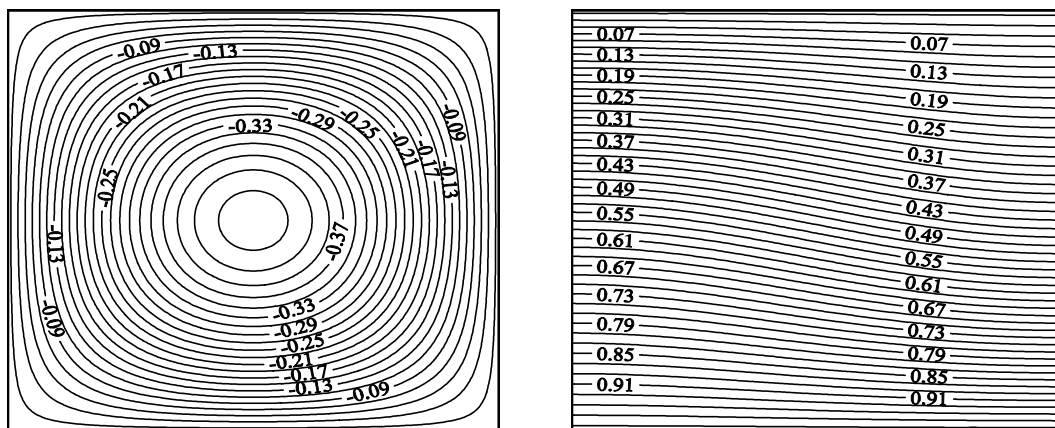
The effect of Rayleigh number and inclination angle on the temperature distribution and flow fields will be discussed.

As mentioned previously, the cases, which received considerable attention, are enclosures heated from below ($\phi = 0^\circ$), and enclosures heated from the side ($\phi = 90^\circ$). The fundamental difference between those two configurations is that in enclosures heated from the side convection is present as soon as a very small ΔT (i.e. small Ra^*) imposed across the enclosure. By contrast, in enclosures heated from below, the imposed ΔT must exceed a critical value (i.e. Ra_c^*) before the first signs of fluid motion are detected.

For the case of $\phi = 0^\circ$, the energy is transported from hot wall to cold wall by pure conduction (i.e. $Nu = 1$) at Rayleigh number less than its critical value. In the conduction regime, the isotherms are almost parallel to isothermal walls. The conduction mode of heat transfer continues until a critical value of Rayleigh number is reached.

In this study, the critical value of Rayleigh number has been found to be equal to 40. This is in a good agreement with the value predicted from the linear theory ($Ra_c^* = 4\pi^2$). At this value the onset of

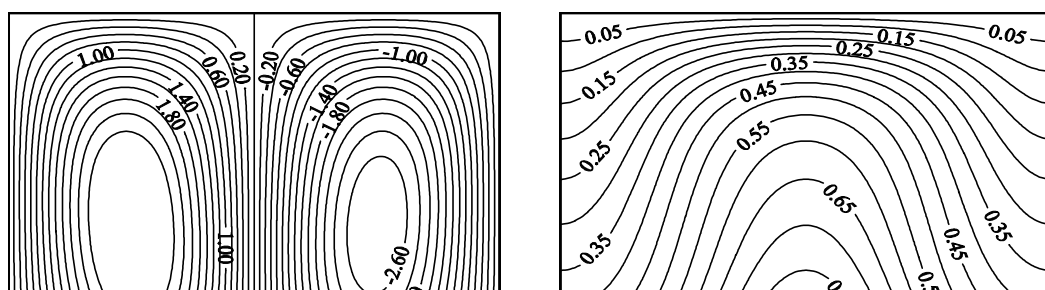
convection begins because of the buoyancy effects. Thus, the flow field comprises a primary cell circulating around the entire enclosure with clockwise (This is an arbitrary direction. It may be counterclockwise), Figure (3) and has a maximum value for the stream function ($\psi_{max} = 0.435$). The small value of ψ_{max} characterizes a very weak convective flow. The isotherms deviate only slightly from those of the pure Conduction state. The extremum value of the stream function becomes larger as Ra^* increase, indicating a more effective motion. In addition, further increase in Ra^* results in changing the direction of the isotherms and change the flow pattern from unicellular to multicellular flow. Figure (4) shows the streamlines at $Ra^* = 100$ and $\phi = 0^\circ$. This flow exhibits two counter-rotating cells, each covering half of the cavity. Both components have the same maximum magnitude (2.79), but are of opposite sign indicating an opposite direction of flow. It also indicates the flow rising slightly in the middle, turning at the top of the cavity, moving adjacent the cold wall, turning, and falling down the insulated wall. The number of cells are increased to three at $Ra^* = 200$ and then reduced to two at $Ra^* = 300$ (see Figures (5) and (6)). The same phenomenon has been noticed by Prasad and Kulacki [15]. □□□□□



(a)

(b)

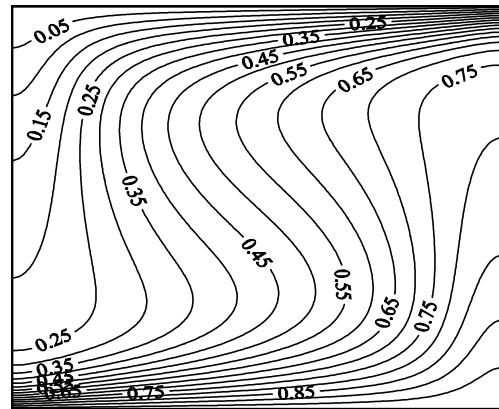
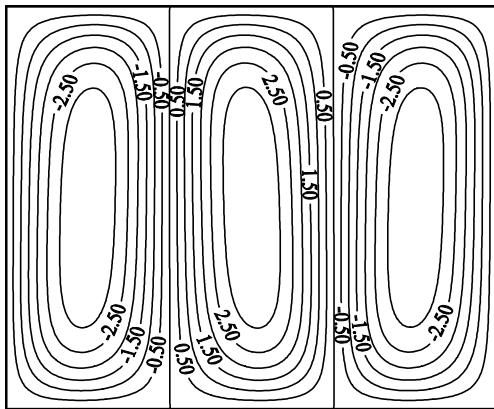
Figure (3) Isograms at $Ra^* = 40$, and $\phi = 0^\circ$: (a) stream function contours; (b) isotherms.



(a)

(b)

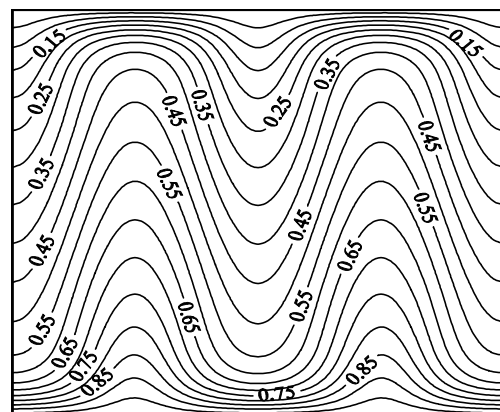
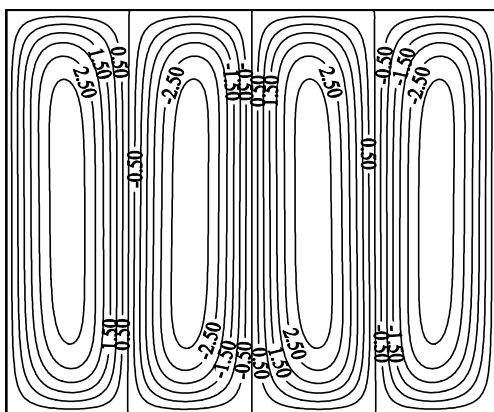
Figure (4) Isograms at $Ra^* = 100$, and $\phi = 0^\circ$: (a) stream function contours; (b) isotherms.



(a)

(b)

Figure (5) Isograms at $Ra^* = 200$, and $\phi = 0^\circ$: (a) stream function contours; (b) isotherms.



(a)

(b)

Figure (6) Isograms at $Ra^* = 300$, and $\phi = 0^\circ$: (a) stream function contours; (b) isotherms.

As the enclosure is inclined with respect to the horizontal line, the convective mode of heat transfer emerge at value of the Rayleigh number much lower than that of horizontal enclosures, similar to those enclosures heated and cooled from vertical sides. This is clearly seen in Figure (7). Based upon the results obtained in this study one can state a criterion for the start of convective flow as:

$$Ra_c^* = A \cdot (\phi)^B \dots\dots\dots(13)$$

Where:

$\phi =$ in radian

$A = 1.30617$

$B = - 0.740221$

For $10^\circ \leq \phi \leq 90^\circ$

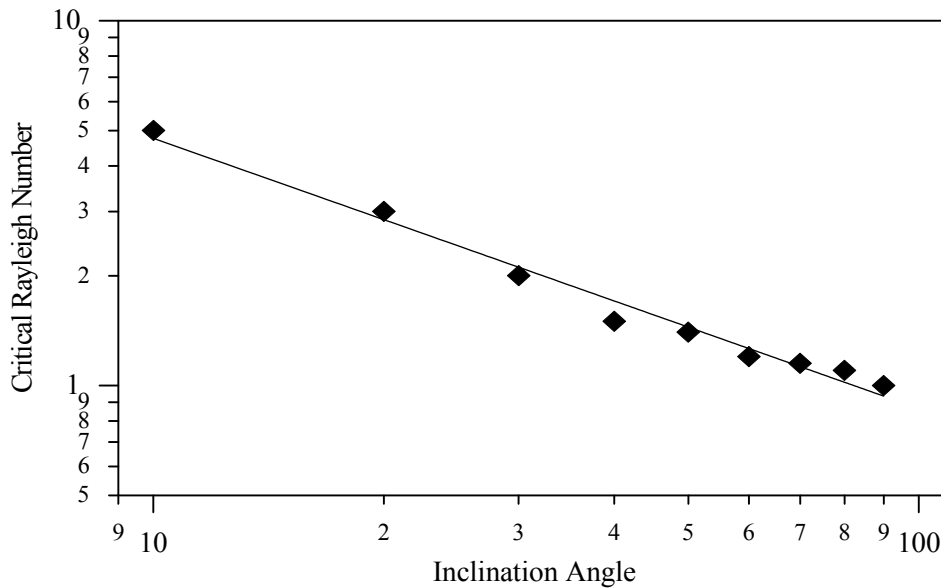
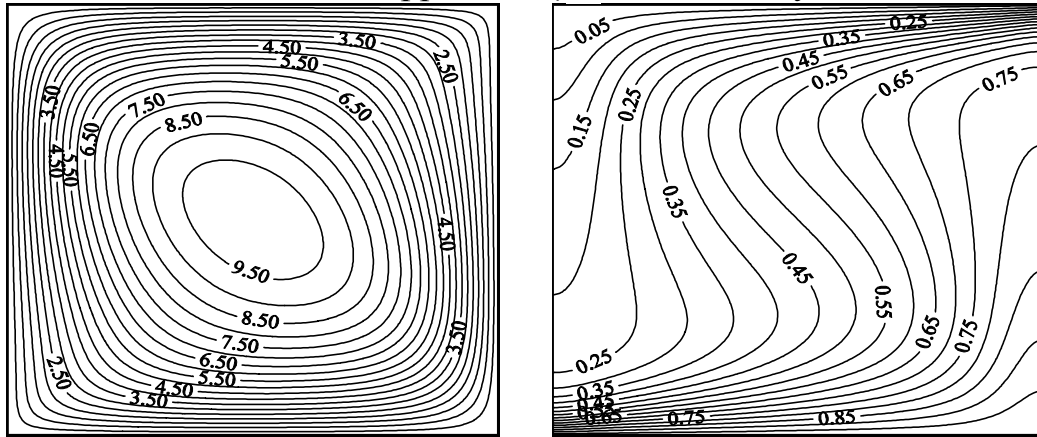


Figure (7) Variation of critical Rayleigh number with the inclination angle ϕ .

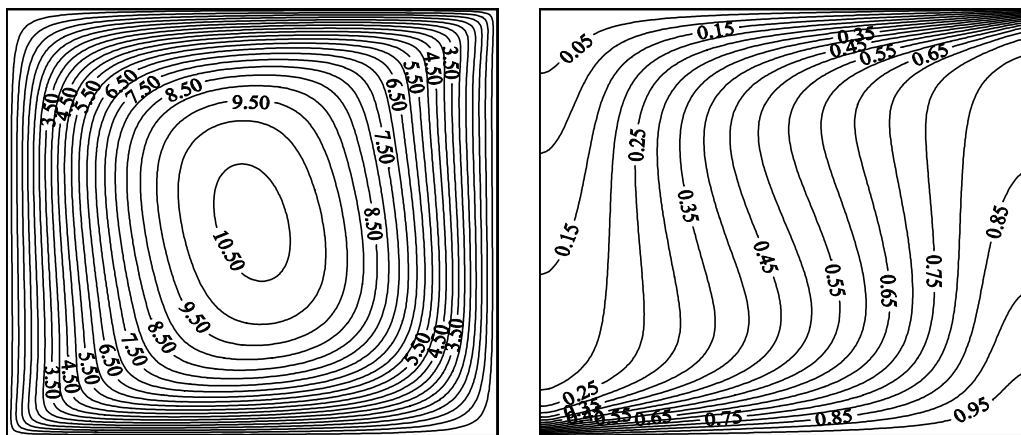
Plots of representative isotherms and streamlines as calculated for $Ra^* = 200$, are presented in Figures (8) to (11) for different values of inclination angle. The flow is mainly single cell flow and the multicellular flow does not appear as ϕ increased beyond 0° .



(a)

(b)

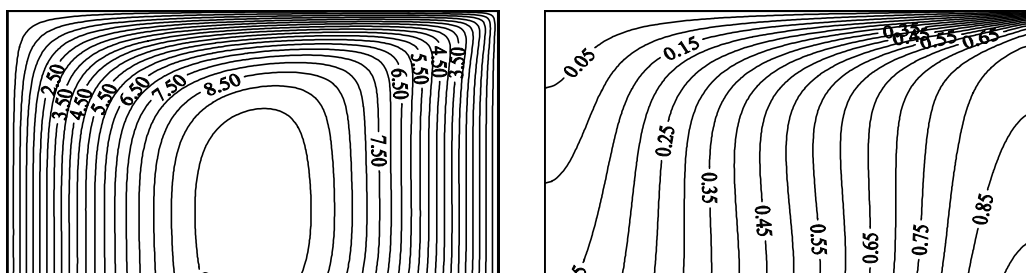
Figure (8) Isotherms at $Ra^*=200$, and $\phi = 10^\circ$: (a) stream function contours; (b) isotherms.



(a)

(b)

Figure (9) Isotherms at $Ra^* = 200$, and $\phi = 40^\circ$: (a) stream function contours; (b) isotherms.

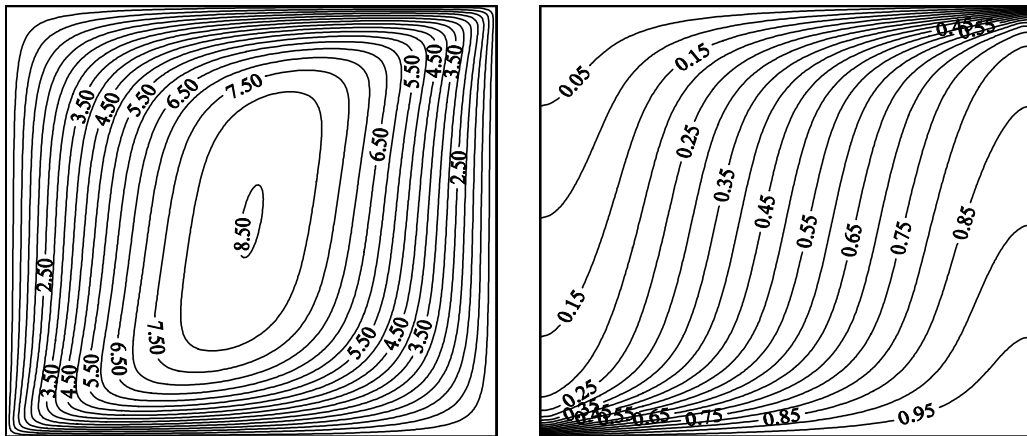


(a)

(b)

Figure (10) Isotherms at $Ra^* = 200$, and $\phi = 70^\circ$: (a) stream function contours; (b) isotherms.

(a) (b)
Figure (10) Isograms at $Ra^* = 200$, and $\phi = 60^\circ$: (a) stream function contours; (b) isotherms.



(a) (b)
Figure (11) Isograms at $Ra^* = 200$, and $\phi = 80^\circ$: (a) stream function contours; (b) isotherms.

The maximum value of the stream function ψ_{max} and the velocity profiles at a position $x=0.5$ as a function of the inclination angle ϕ and Rayleigh number Ra^* are presented in Figures (12) and (13), respectively.

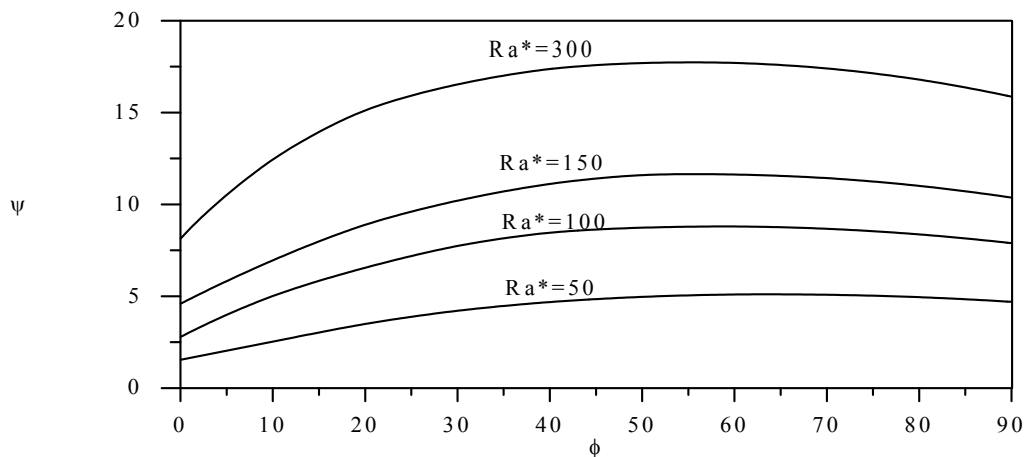


Figure (12) Variation of ψ_{max} with the inclination angle (ϕ) for different values of Rayleigh number (Ra^*).

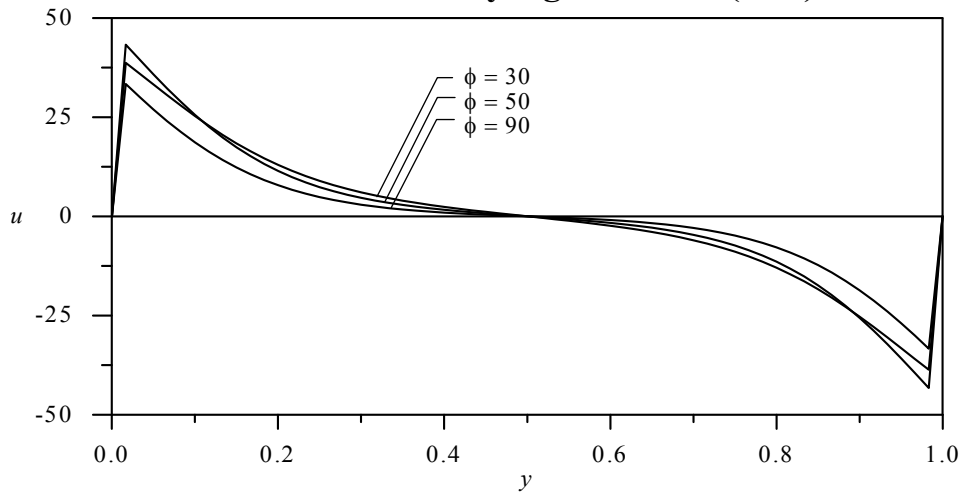


Figure (13) Velocity profiles (u) at vertical centerline ($x = 0.5$) for different values of inclination angle (ϕ) at $Ra^*=100$.

The curves illustrate the fact that the convection becomes vigorous as the orientation angle of the cavity is increased. It is observed from Figure (12) that the curves for ψ_{max} reach a maximum value when the angle of inclination in the range (50° to 60°) from the horizontal line, depending upon Rayleigh number. From Figure (13) it is seen that the velocity is maximum at a position $\phi = 50^\circ$ for $Ra^*=100$.

Heat Transfer

As mentioned above, heat transfer results are presented in term of average hot wall Nusselt number (Nu). Figure (14) show the variation of Nusselt number versus Rayleigh number with different values of inclination angle. It is clear that Nu equal to one in the conduction regime (i.e. at $Ra^* \leq Ra_c^*$). The reason is that the viscous force is greater than the buoyancy force therefore the heat is transported by conduction as discussed previously. It is also seen that for short range of Rayleigh number after Ra_c^* , the rate of increase in Nu against Ra^* is

relatively small. Then, Nu increases rapidly as Ra^* increases expressing the existence and increase of convective heat transfer.

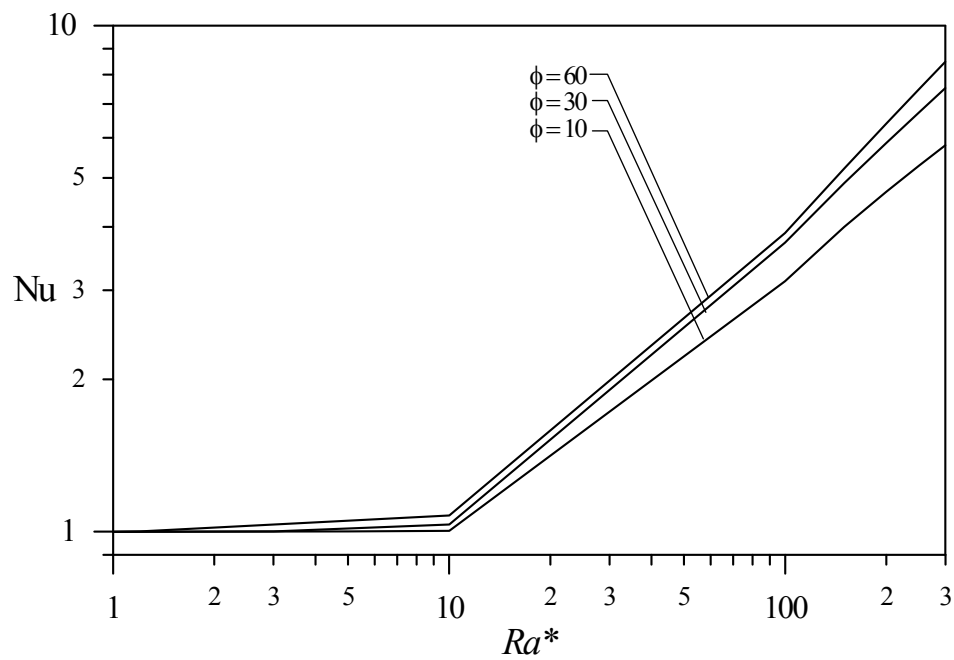


Figure (14) Nusselt number (Nu) vs. Rayleigh number (Ra^*) for different inclination angles.

Figure (15) represent the relationship between the average Nusselt number and inclination angle for Rayleigh numbers of $Ra^* = 100, 150,$

and 300, respectively. The inclination angle is seen to have a dominant effect on the Nu for a given Ra^* . As shown, the value of Nu increases with increasing ϕ above 0° (heated from below) passes through a peak and then begins to decrease. A similar trend has been reported by Ozoe et al. [16] in the case of inclined fluid cavities containing two opposite isothermal surface maintained at different temperature. Also, a similar behavior has been seen experimentally in porous medium by Inaba et al. [6]. The value of ϕ at which Nu reached the maximum is changed as Ra^* increases. It falls in the range of inclination angle of $50^\circ \leq \phi \leq 57^\circ$. For example, at $Ra^*=100$ the value of ϕ_{max} for which Nu is maximum, is about 50° while ϕ_{max} is approximately 53° for $Ra^*=300$. This is in coincidence with the results obtained for the maximum stream function. It is also noticed that the effect of inclination angle on Nusselt number is more pronounced as the Rayleigh numbers increase.

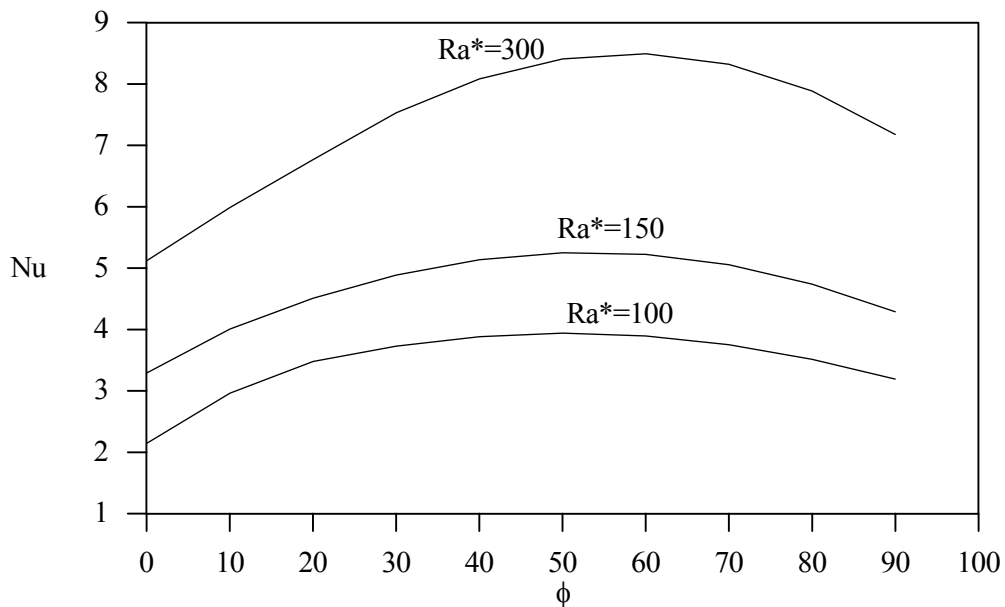


Figure (15) Variation of Nusselt number vs. inclination angle for different values of Rayleigh number.

Correlation Equation

In prior sections, the dependency of Nusselt number on the investigation parameters (i.e., Rayleigh number, and inclination angle) has been illustrated. Therefore, attempts have been made to correlate Nusselt number with those parameters. Those attempts were not

successful because the obtained correlation was not suitable for precise data description. So that, correlation of Nusselt number with Rayleigh number has been produced for each inclination angle as:

$$Nu = c (Ra^*)^d \dots\dots\dots(14)$$

The coefficients of equation (14) for each inclination angle are presented in table (2).

Const.	Inclination Angle (°)									
	0	10	20	30	40	50	60	70	80	90
c	0.072	0.159	0.164	0.161	0.157	0.148	0.140	0.131	0.124	0.120
d	0.741	0.637	0.657	0.677	0.695	0.769	0.721	0.728	0.728	0.716

Table (2) Constant coefficients of equation (14).

The above correlation is acceptable in the range of Rayleigh number (0 - 300), and inclination angle (0° - 90°). To ensure that these approximation correlations are usable, the correlation coefficient R had been obtained for each equation. The minimum value of R was (0.94), that means these approximate equations are good for predicting the value of Nusselt number. Figure (16) shows the results with curve fit for some cases.

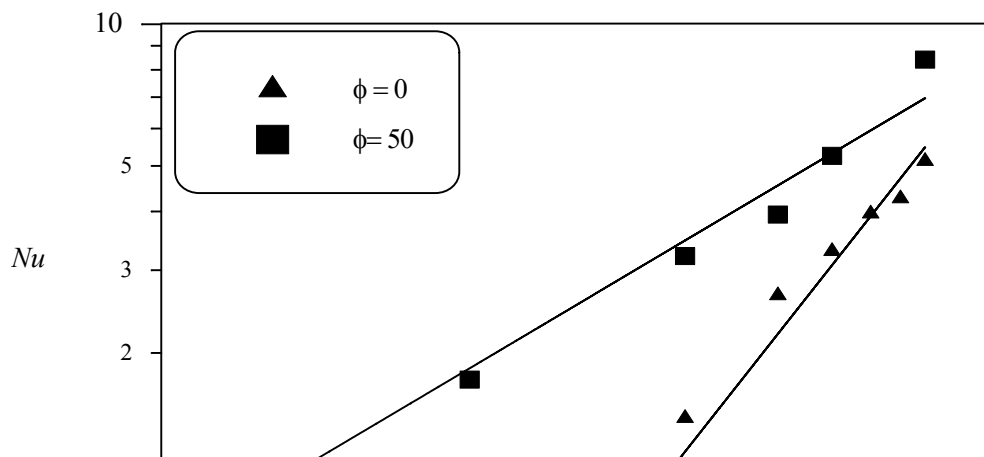


Figure (16) Variation of Nusselt number vs. Rayleigh number with curve fits for different values of inclination angle.

Conclusions

The problem of natural convection in a two-dimensional, inclined porous layer with uniform temperature on two opposite walls while the other walls are insulated has been studied numerically. The main conclusions of the present study are:

1. For cavities maintained in the horizontal position the critical Rayleigh number for the onset of natural convection Ra_c^* can be predicted from the linear theory. As the angle of inclination ϕ increases beyond 0° the value of the value of Ra_c^* decreases. Thus, the value of Ra_c^* , as a function of inclination angle ϕ , can be calculated from equation (13).
2. The orientation of the cavity has, for a given Rayleigh number, a large effect on the heat transfer rate. The maximum heat transfer occurs when the enclosure inclination between $(50^\circ \leq \phi \leq 57^\circ)$. As the Rayleigh number increase the angle at which maximum energy transfer takes place ϕ_{\max} shifts towards higher values of ϕ . Equation (14) and table (2) can be used to calculate the rate of heat transfer as a function of Ra^* , ϕ .

References

1. Kaneko, T., Mohtadi, M. F., and Aziz, K., "An Experimental Study of Natural Convection in Inclined Porous Media," Int. J. Heat Mass Transfer, 17, pp.485-496, 1974.
2. Horton, C. W., and Rogers, F. T., "Convection Currents in a Porous Medium," J. Appl. Phys., 16, pp.367-370, 1945.
3. Katto, Y., and Masuoka, T., "Criterion for the Onset of Connective Flow in a Porous Medium," Int. J. Heat Mass Transfer, 10, pp.297-309, 1967.
4. Bories, S. A., and Combarous, M.A., "Natural Convection in a sloping Porous Layer," J. Fluid Mech., 57, pp.63-79, 1973.
5. Oosthuizen, P. H., and Paul, J. T., "Natural Convection in an Inclined Partitioned Square Cavity Half-Filled with a Porous Medium," 24th. ASME Heat Transfer Conference, Pittsburgh, pp.1-10, 1987.
6. Inaba, H., Sugawara, M., and Paul, J. T., "Natural Convection Heat Transfer in an Inclined Porous Layer," Int. J. Heat Mass Transfer, 31, pp.1365-1374, 1988.
7. Mbaye, M., Bilgen, E., and Vasseur, P., "Natural Convection Heat Transfer in an Inclined Porous Layer Boarded by a Finite-Thickness Wall," Int. J. Heat Fluid Flow, 14, pp.284-291, 1993.
8. Chan, B. K. C., Ivey, C. M., and Barry, J. M., "Natural Convection in Enclosed Porous Media with Rectangular Boundaries," J. Heat Transfer, 2, pp.21-27, 1970.
9. Burns, P. J., Chow, L. C., and Tien, C. L., "Convection in Vertical Slot Filled with Porous Insulation," Int. J. Heat Mass Transfer, 20, pp.919-926, 1974.
10. Bejan, A., and Tien, C. L., "Natural Convection in a Horizontal Porous Medium Subjected to an End-to-End Temperature Difference," J. Heat Transfer, 100, pp.191-198, 1978.
11. Bejan, A., "Natural Convection Heat Transfer in a Porous Layer with Internal Flow Obstructions," Int. J. Heat Mass Transfer, 26, pp.815-822, 1983.
12. Cheng, P., "Heat Transfer in Geothermal Systems," Adv. Heat Transfer, 14, pp.1-105, 1978.
13. Dawood, A. S., "Steady Three-Dimensional Natural Convection in Porous Media Via Multigrid Method," Ph. D. Dissertation, Dept. of Mech. Eng., Colorado State University, 1991.
14. Bejan, A., Convection Heat Transfer, Wiley-Interscience Publication, Joun Wiley & Sons, Inc., 1995.

15. Prasad, V., and Kulacki, F. A., "Convective Heat Transfer in a Rectangular Porous Cavity - Effect of Aspect Ratio on Flow Structure and heat Transfer," J. Heat Transfer, 106, pp.158-165, 1984.
16. Ozoë, H., Sayama, H., and Churchill, S. W., "Natural Convection Patterns in a Long Inclined Rectangular Box Heated from Below," Int. J. Heat Mass Transfer, 20, pp. 123-129, 1977.